Progress in Reaction Kinetics and Mechanism. Vol. 37, pp. 249–262. 2012
doi: 10.3184/146867812X13377012276288 1468-6783 © 2012 Science Reviews 2000 Ltd

RESEARCH PAPER

Kinetic studies of isothermal decomposition of unirradiated and γ-irradiated gallium acetylacetonate: new route for synthesis of gallium oxide nanoparticles

R.M. Mahfouz[a]*, Kh.M. Al-Khamis[a], M.R.H. Siddiqui[a], N.S. Al-Hokbany[a], I Warad[b] and N.M. Al-Andis[a]

[a]*Department of Chemistry, College of Science, King Saud University, PO Box 2455, Riyadh-11451, Saudi Arabia*

[b]*Department of Chemistry, AN-Najah National University, PO Box 7, Nablus Palestine Territories*

**E-mail: rmhfouz@ksu.edu.sa*

ABSTRACT

Isothermal decomposition of unirradiated and γ-irradiated gallium acetylacetonate $Ga(acac)_3$ with 10^3 kGy total γ-ray dose was carried out in static air. The isothermal operating temperatures were 160, 170, 180 and 190°C. The kinetics of decomposition were followed using both model-fitting and model-free approaches. The results of model fitting application on the investigated data showed that the decomposition behaviour was best described by phase-boundary controlled reaction (R_2). Kinetic parameters of the decomposition process were calculated and evaluated. Analysis of the data using model free approach signifies the dependency of E_a on extent of conversion (α). Pre-γ-irradiation of gallium acetylacetonate $Ga(acac)_3$ with 10^3 kGy total γ-ray dose has almost no effect on the kinetic parameters.

KEYWORDS: gallium acetylacetonate, γ-irradiation, isothermal decomposition

1. INTRODUCTION

Thermal treatment of inorganic substances has a great synthetic potential as it may convert simple compounds into more complex material, such as ceramics, catalysts and glasses, and could lead to metal or oxide nanoparticles displaying a very narrow size distribution [1]. Many recent studies on the thermal decomposition of inorganic solids have included measurements on samples that were exposed to radiation prior to heating with the aim of investigating the effect

of ionising radiation on the kinetics and thermal decomposition behaviour of inorganic compounds [2–7]. Gallium(III) acetylacetonate, $Ga(acac)_3$ is a suitable metallic organic compound for the preparation of Ga_2O_3. Monoclinic gallium oxide (β-Ga_2O_3) is chemically and thermally stable compound with a wide-band gap of 4.9 eV [8]. It exhibits conductive and a photoluminescence properties [9]; it is a promising candidate for application as a transparent conducting material and in next generation optoelectronic devices. Ga_2O_3 has recently attracted interest due to its applications ranging from gas sensors [10,11] and nano-structural materials to important agents in catalysis [12–15]. Gallium oxide has been used as an insulating barrier for spin-dependent tunneling junction [16].

In continuation of our studies on the thermal decomposition of acetyl acetonate compounds [1,2,17], we report here the results of our studies on the thermal decomposition behaviour of unirradiated and γ-irradiated $Ga(acac)_3$. This was investigated in static air in order to shed more light on the kinetics of thermal decomposition of $Ga(acac)_3$ and the role of ionising radiation on the thermal behaviour of $Ga(acac)_3$.

2. EXPERIMENTAL

Gallium acetylacetonate (Aldrich Ltd) was used without further purification. For the thermal experiment, a TGA-7, Perkin-Elmer thermogravimetric analyser was used. The sample was maintained at 10 ± 0.1 mg and the decomposition was followed in static air using isothermal and dynamic thermogravimetric techniques. Under isothermal conditions, four temperatures (160, 170, 180 and 190°C) were selected for measurements and the heating rate was 10°C min^{-1}. For irradiation, samples were encapsulated under vacuum in glass vials and exposed to successively increasing doses of radiation at constant intensity using a Co-60 γ-ray cell 220 (Nordion INT–INC, Ontario, Canada) at a dose rate of 10^4 Gy h^{-1}. The source was calibrated against a Fricke ferrous sulfate dosimeter. The dose rate in the irradiation samples was calculated by applying appropriate corrections on the basis of both the photon mass attenuation and energy absorption coefficient for the sample and dosimeter solutions [18].

The fraction decomposed or the extent of conversion of α was calculate as

$$\alpha = \frac{mo - m}{mo - m_f}$$

where mo, m, m_f are the initial, actual and final sample masses, respectively. The IR spectra were recorded as a KBr pellets using a Perkin-Elmer 1000 FT-IR spectrophotometer, XRD was carried out on a Siemens D 5000 X-ray diffractometer using a nickel filter (Cu Kα, $\lambda = 1.5418$ Å).

3. THEORY

A single-step process for solid state decomposition has the following kinetic equation

$$\frac{d\alpha}{dt} = K(T)\,f(\alpha) \tag{1}$$

where α is the extent of conversion, t is the time, T is the temperature, $K(T)$ is a temperature dependent reaction rate constant, and $f(\alpha)$ is a kinetic dependent model function.

The Arrhenius equation generally expresses the explicit temperature dependency of the rate constant as

$$\frac{d\alpha}{dt} = A\exp\left(\frac{-E_a}{RT}\right) f(\alpha) \tag{2}$$

The A, E, and $f(\alpha)$ are called the ''kinetic triplet'' that can characterise a unique decomposition reaction Some of the reaction models for solid state reactions are listed in Table 1. Under non-isothermal conditions in which a sample is heated at a constant rate, the explicit time dependence in Eqn (1) is eliminated through the transformation

$$\frac{d\alpha}{dt} = \frac{A}{\beta}\exp\left(\frac{-E_a}{RT}\right) f(\alpha), \tag{3}$$

where $\beta = dT/dt$ is the heating rate.

3.1 Model-fitting approach

Rearrangement and integration of Eqn (1) for isothermal conditions gives

$$g_j(\alpha) = K_j(T)t \tag{4}$$

where $g(\alpha) = \int_0^\alpha [f(\alpha)]^{-1} d\alpha$ is the integrated form of the reaction model. The subscript j has been introduced to emphasise that substituting a particular reaction model into Eqn (4) gives the corresponding rate constant.

A plot of $g(\alpha)$ *versus* t should give a straight line if the corrected form of $g(\alpha)$ is selected, and the slope of the plot gives the rate constant. The function $g(\alpha)$ depends on the mechanism controlling the reaction and on the size and shape of reaction particles [19]. In a diffusion-controlled reaction, D_1 is the function for a one-dimensional diffusion process governed by a parabolic law with constant diffusion coefficient, D_2 is that for a two-dimensional diffusion-controlled process into a cylinder, D_3 is Jander's equation for a diffusion-controlled reaction in a sphere, and D_4 is the function for a diffusion-controlled reaction starting on the exterior of a spherical particle. In phase-boundary-controlled reactions, the reaction is controlled by movement of an interface at a constant velocity and nucleation occurs virtually instantaneously. Then, the equation relating α and t is the R_2 function for a circular disc reaction from the edge inward, and the function R_3 is for a sphere reaction from the surface inward. If the solid-state reaction follows first-order kinetic (F_1 function) then the rate-determining step is the nucleation process and there is an equal probability of nucleation at each active site. In a phase-boundary reaction, it is assumed that the nucleation step occurs instantaneously so that the surface of each particle is covered with a layer of the product. Nucleation of the reactant, however, may be a random process, not followed by rapid surface growth. As the nuclei grow larger they must eventually impinge on one another, so that the growth ceases where they touch.

The rate constant can be determined at various temperatures, T_i, and then the Arrhenius parameters can be estimated from the Arrhenius plots of the rate constants as follows

$$\ln k_j(T_i) = \ln A_j - \frac{E_{a,j}}{RT_i} \tag{5}$$

To choose an appropriate reaction model, one can plot α as a function of a reduced time variable t/t_α, where t_α is the time required to reach a specified conversion (*e.g.* $\alpha = 0.9$). this method is used extensively in solid state kinetics [20]. The goodness of fit of the theoretical RTP (reduced time plot) to the experimental one can be judged by the residual sum of squares [19]

$$S_j^2 = \frac{1}{n-1}\sum_{i=1}^{n}\left(\frac{t_i}{t_{0.9}} - \frac{g_i(\alpha_i)}{g_i(0.9)}\right)^2 \tag{6}$$

3.2 Model-free approach

A model-free equation using isothermal kinetic data can be denoted by

$$-\ln t_{\alpha,t} = \ln\left(\frac{A_\alpha}{g_{(\alpha)}}\right) - \left(\frac{E_a}{R}\right)\frac{1}{T_i} \tag{7}$$

where E_a is evaluated from the slope of the plot $-\ln t_{\alpha,I}$ against T_i^{-1}.

Applying the above equation to the isothermal kinetic data, the E_a value is obtained as a function of α.

4. RESULTS AND DISCUSSION

Figure 1 depicts the simultaneous TG and DTA curves for $Ga(acac)_3$ from ambient up to 600°C. For unirradiated $Ga(acac)_3$ the TG exhibits first a slow degradation step in the temperature range of 50 – 100°C with an endothermic peak maximised at 75°C due to the escape of moisture and volatile impurities. Then there is a next sudden collapse due to simultaneous melting, volatilisation and degradation of $Ga(acac)_3$ with an endothermic peak maximised at 220°C. The next three smaller endothermic steps in the temperature range of 230 – 280°C, depict the slow degradation of intermediates. These three endothermic peaks were followed by a sharp exothermic weight gain with an exothermic peak maximised at 310°C attributed to oxidation process and formation of Ga_2O_3 as a final solid residue product. Comparing the theoretically calculated weight losses values with

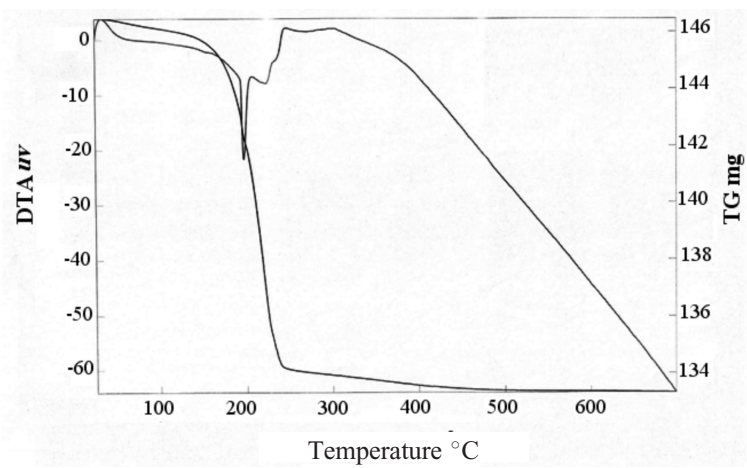

Figure 1 Simultaneous TG/DTA curves of unirradiated $Ga(acac)_3$.

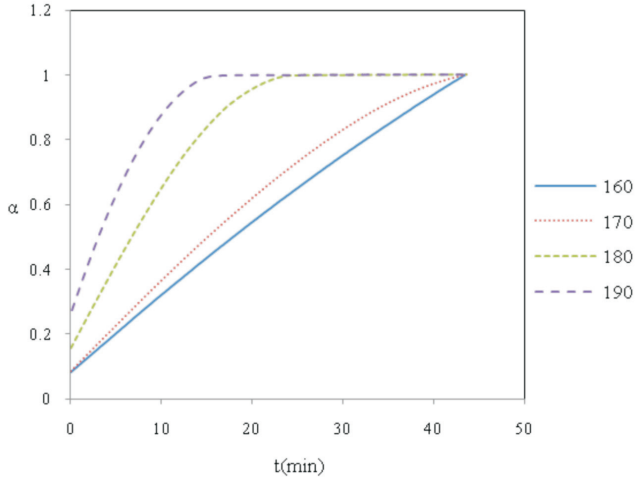

Figure 2 Fractional decomposition, α *versus* time (*t*) curves for isothermal decomposition of unirradiated $Ga(acac)_3$.

the experimentally ones, we come to conclusion that the main decomposition step could be attributed to the loss of one molecule of (CH_3COCH_3) and one molecule of ($CH_3COCH_2COCH_3$). This results in the formation of non-stoichiometric coordinated species of the type $[Ga(OH)CHOO]^+$ which slowly disproportionate with three consecutive chemical processes to form Ga(0) and (CH_3COOH). Ga(0) is readily oxidised to form Ga_2O_3 ($solid_1 - solid_2$ amorphous-crystalline transformation) as the final solid residue. Its structure was confirmed by its IR and XRD spectra. CH_3COOH easily decomposes to form CH_4 and CO_2 [21].

Typical TG and DTA curves of γ-irradiated $Ga(acac)_3$ with a total dose (10^3 kGy) showed almost the same decomposition behaviour as the unirradiated one without any significant changes observed in case of irradiated sample.

Figure 2 shows the isothermal kinetic results, *i.e.* α *versus* time plots, for unirradiated $Ga(acac)_3$. Using Eqn (4), the different $g_i(\alpha)$ models listed in Table 1 are plotted against *t*. The isothermal operating temperatures were selected to be 160, 170, 180 and 190°C. The γ-irradiated $Ga(acac)_3$ sample gave similar plots.

The results indicate that the best fits to isothermal data were obtained using R_2 (the phase-boundary controlled reaction) model as shown in Figure 3 for both unirradiated $Ga(acac)_3$. Similar plot was obtained for γ-irradiated $Ga(acac)_3$. The kinetic parameters E_a and $\ln A$ were calculated from the slopes and intercepts of the straight lines obtained and are listed in Table 1 together with the kinetic parameters evaluated using other $g_i(\alpha)$ models.

Table 1 Arrhenius parameters for isothermal decomposition of unirradiated and γ-irradiated (10^3 kGy) $Ga(acac)_3$

Model	Unirradiated sample			Irradiated sample with total dose 10^3 kGy		
	E_a	$\ln A_j$	r_j	E_a	$\ln A_j$	r_j
D_1	68.86	15.2	0.97	57.89	12.11	0.987
D_2	71	15.59	0.919	63.32	13.41	0.95
D_3	69.28	14.29	0.805	54	9.981	0.851
R_2	66.78	14.36	0.984	59.61	12.33	0.996
R_3	69.97	14.98	0.965	62.51	12.87	0.984
A_2	68.09	15.31	0.983	60.12	13.06	0.992
A_3	45.64	8.567	0.982	62.51	12.87	0.984

No significant changes were observed in the Arrhenius kinetic parameters estimated for unirradiated and γ-irradiated $Ga(acac)_3$.

Figure 4 shows the reduced time plots of the theoretical and experimental isothermal data at the isothermal operating temperatures of 160, 170, 180 and 190°C, with model R_2 given the best agreement with curve 12. Statistical analysis by the residual sum of squares, Eqn (6), indicated that sets of data for unirradiated and γ-irradiated $Ga(acac)_3$ are also well-modelled by the R_2 function.

Application of the model-free isoconversional method, Eqn (7), to the isothermal decomposition data for both unirradiated and γ-irradiated $Ga(acac)_3$ (total dose 10^3 kGy) enables the determination of E_a as a function of α, and the results are shown in Figure 5. A significant decrease can be observed in the value of E_a with an increase of α values up to $\alpha = 0.5$ where almost no detectable changes were recorded for either the unirradiated or the γ-irradiated $Ga(acac)_3$.

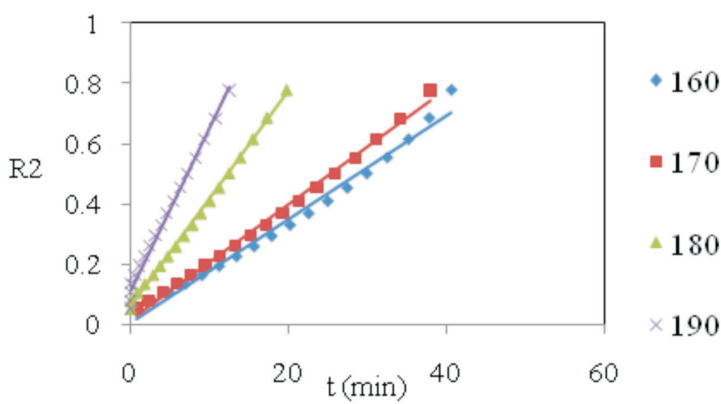

Figure 3 Isothermal decomposition curves of unirradiated $Ga(acac)_3$.

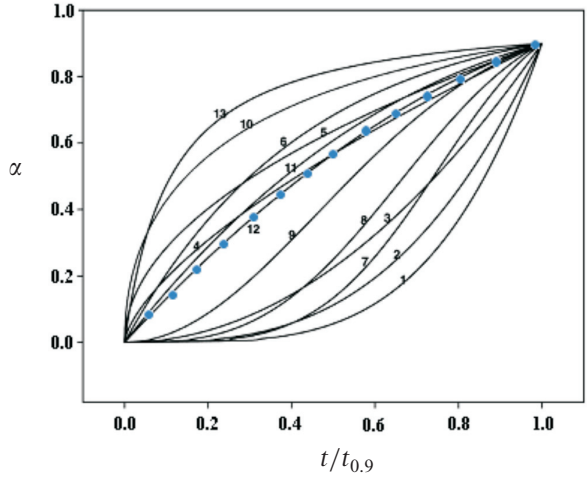

Figure 4 Reduced time plots for the reaction models (as enumerated in Table 1) and isothermal experimental data (—●—●—) for $Ga(acac)_3$.

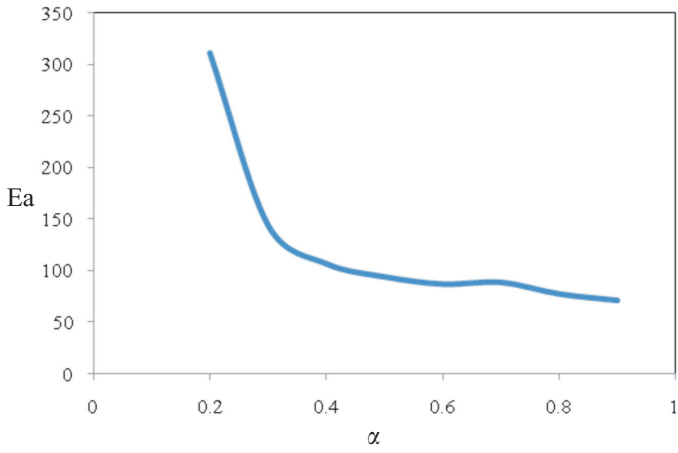

Figure 5 Dependence of the activation energy on the extent of unirradiated $Ga(acac)_3$, conversion determined using model-free isoconversional method for isothermal data.

5. IR, XRD MEASUREMENTS

The IR spectrum of γ-irradiated $Ga(acac)_3$ with 10^3 kGy total γ-ray dose, displays the main characteristic peaks of the acetylacetonate ligand. Neither the appearance of a new band nor the disappearance of an old band was recorded because of the γ-irradiation. The band assigned to ν Ga—O bond at 654 cm^{-1} was more affected

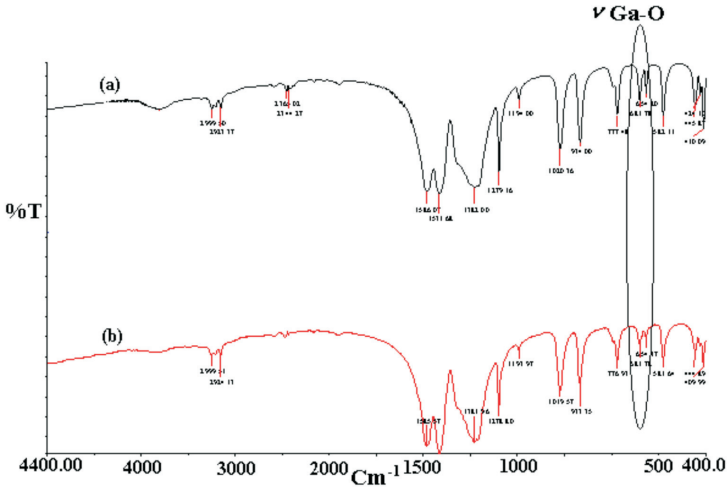

Figure 6 IR spectra of (**a**) unirradiated $Ga(acac)_3$ and (**b**) γ-irradiated $Ga(acac)_3$ with a total dose of 10^3 kGy.

by irradiation than any other band in the spectrum. The decrease in the intensity of this band achieved by irradiation is shown in Figure 6. This decrease in the intensity could be attributed to bond scission and degradation caused by γ-irradiation.

XRD patterns of unirradiated and γ-irradiated $Ga(acac)_3$ both showed the same characteristic features of a monoclinic system without any significant changes occurring as a results of γ-irradiation with the 10^3 kGy total γ-ray dose.

XRD and IR measurements were used to follow the formation of Ga_2O_3 nanoparticles by calcination of both unirradiated and γ-irradiated $Ga(acac)_3$ at different temperatures and time intervals. From these experiments we concluded that calcination of $Ga(acac)_3$ at 900°C for 6 hours led to the formation of Ga_2O_3 nanoparticles as was demonstrated by XRD, FTIR, SEM and TEM measurements.

Figure 7 showed the XRD pattern of the gallium oxide nanoparticles. The sharp diffraction peaks in the pattern can be indexed to a monoclinic structure, which are in good agreement with the reported data of β-Ga_2O_3.

Figure 8 showed the FTIR spectrum of the samples calcined at 900°C for 6 hours. The characteristic bands at 669.99 and 452.46 Cm^{-1} were attributed to *ν*Ga—O of Ga_2O_3.

Figure (9a) shows the SEM images of Ga_2O_3 nanoparticles obtained by thermal decomposition of unirradiated $Ga(acac)_3$ under the conditions mentioned previously. The image displays nearly spherical particles with diameters in the

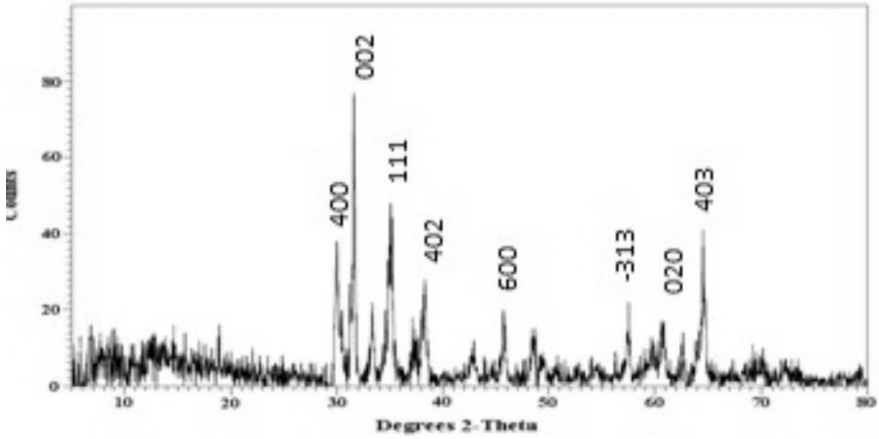

Figure 7 XRD pattern of β-Ga_2O_3 nanoparticles obtained by calcination at 900°C for 6 hours.

range of 18 – 62 nm. The image recorded some aggregation of the particles and could be attributed to electron beam irradiation during SEM measurements. The SEM image for the γ-irradiated $Ga(acac)_3$ sample, as shown in Figure (9b), displays more dispersed nanoparticles, without a change in the morphology of the sample compared with the unirradiated one. However, small holes were observed for this sample which were not present before. This might be due to the damage and point defects created by irradiation.

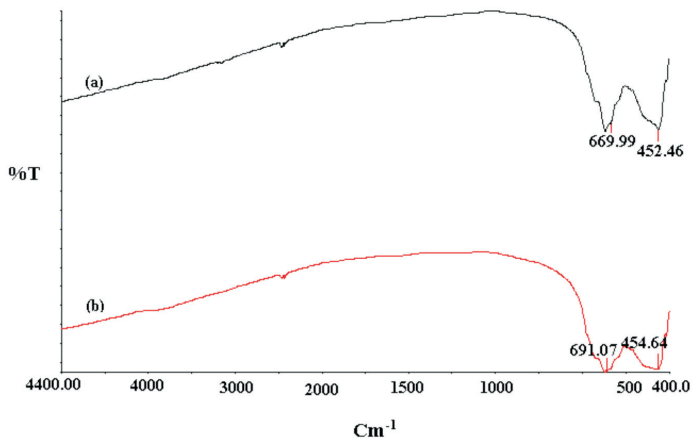

Figure 8 FTIR spectrum of β-Ga_2O_3 nanoparticles obtained by calcination at 900°C for 6 hours (**a**) unirradiated sample (**b**) γ-irradiated sample with a total dose of 10^3 kGy.

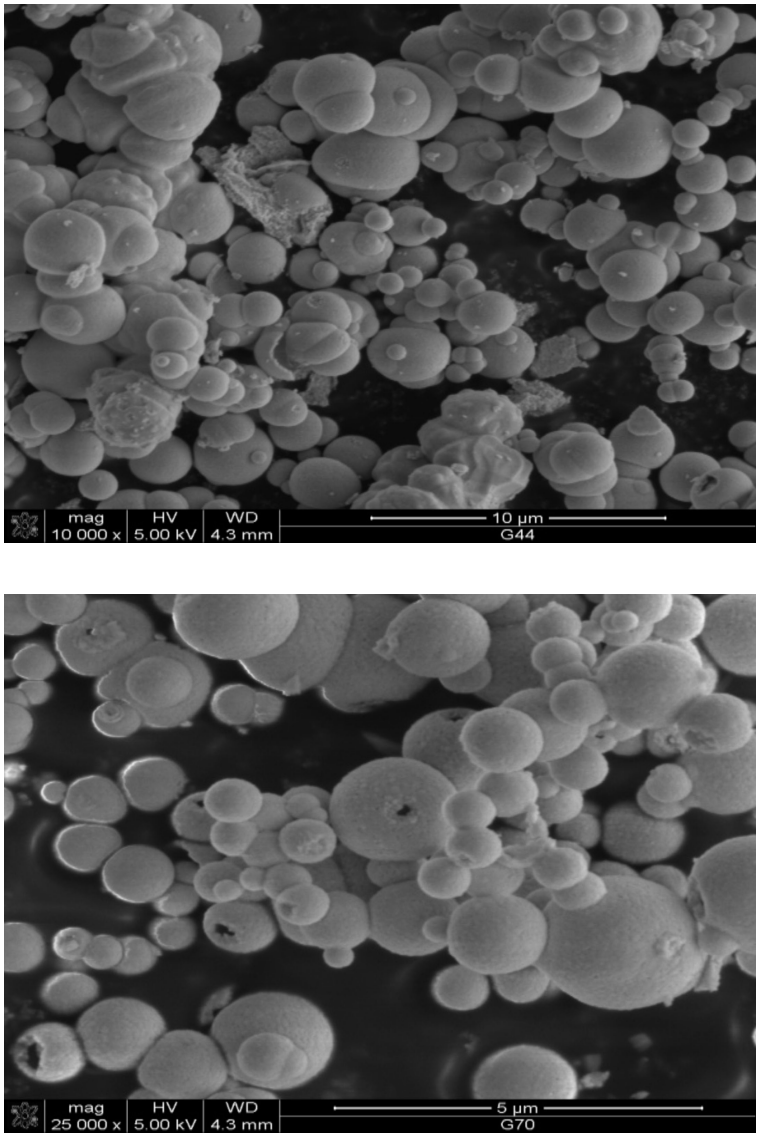

Figure 9 SEM image of β-Ga_2O_3 nanoparticles obtained by calcination at 900°C for 6 hours (**a**) unirradiated sample (**b**) γ-irradiated sample with a total dose of 10^3 kGy.

Figure 10 shows the TEM images of Ga_2O_3 nanoparticles obtained by thermal decomposition of unirradiated and γ-irradiated $Ga(acac)_3$ under the condition mentioned previously. The images display the cubic close packing system of β-Ga_2O_3.

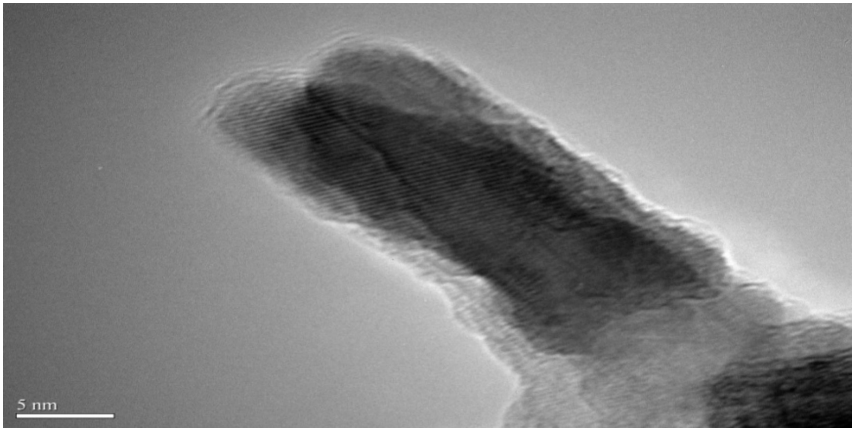

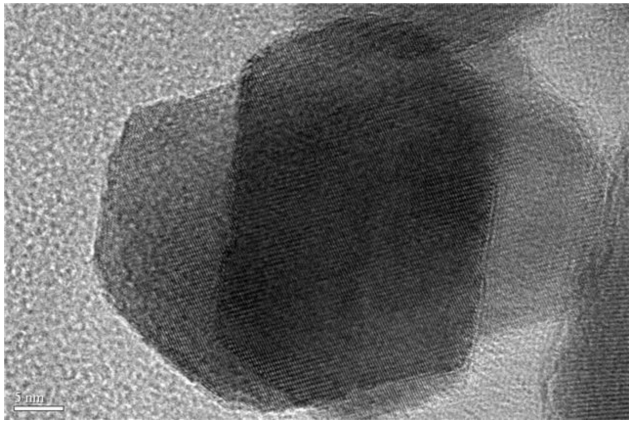

Figure 10 TEM image of the β-Ga_2O_3 nanoparticles obtained by calcination at 900°C for 6 hours (**a**) unirradiated sample (**b**) γ-irradiated sample with a total dose of 10^3 kGy.

Comparable sol-gel experiments using $Ga(acac)_3$ as the precursor were performed under different calcination temperatures in presence of gelatin and the results are shown in Figure 11.

6. CONCLUSIONS

We have presented model-fitting and model-free approaches for the kinetic analysis of isothermal decomposition of unirradiated and γ-irradiated $Ga(acac)_3$ with a total dose of 10^3 kGy. The results show that there is no significant change in the behaviour, mechanism, and kinetic parameters of the thermal decomposi-

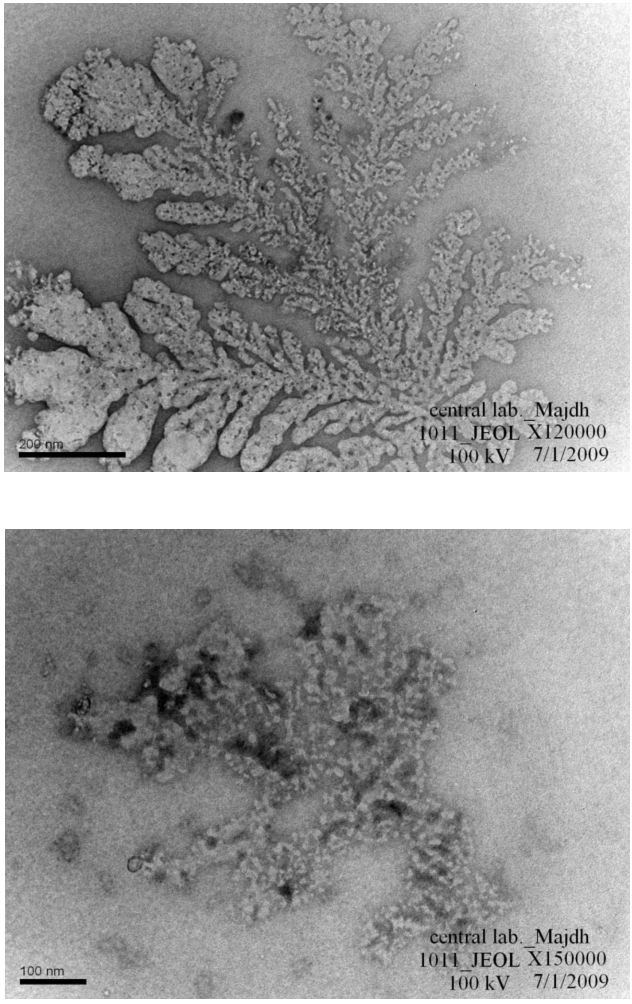

Figure 11 TEM image of Ga_2O_3 prepared by sol-gel method using (**a**) unirradiated $Ga(acac)_3$ (**b**) γ-irradiated sample with a total dose of 10^3 kGy.

tion between unirradiated and γ-irradiated samples of $Ga(acac)_3$. Calcination of unirradiated and γ-irradiated samples of $Ga(acac)_3$ at 900°C for 6 h led to the formation of the β-Ga_2O_3 nanostructure. Compared with our earlier work on non-isothermal decomposition [17] of Ga_2O_3, the isothermal results led to a different kinetic model which is R_2. For non-isothermal studies the kinetic model was D_2. It should be noted that the non-isothermal analysis gives more reliable results than the isothermal data, since changing the temperature is one of the most important factors affecting the thermal behaviour of inorganic solids [20].

Further experiments and discussions concerning preparation of Ga_2O_3 nanoparticles using both solid state thermal decomposition and sol-gel methods starting from different Ga-precursors are now in progress at our laboratory and will be published in a separate publication.

ACKNOWLEDGEMENT

This work is supported by the Research Center, College of Science, King Saud University, Riyadh, Kingdom of Saudi Arabia.

REFERENCES

[1] Mahfouz, R.M., Siddiqui, M.R.H., Al-Ahmari, Sh.A. and Alkayali, W.Z. (2007) *Prog. React. Kinet. Mech.*, **32**, 1 – 27.
[2] Mahfouz, R.M., Al-Ahmari, Sh.A., Al-Fawaz, A.M., Al-Othman, Z., Warad, I.Kh. and Siddiqui, M.R.H. (2009) *Radiat. Effects Defects Solids*, **164**, 266 – 275.
[3] Van Der Voort, P., White, M.G. and Vansant, E.F. (1998) *Langmuir*, **14**, 106 – 112.
[4] Vasvári, G., Hajdu, I.P. and Gál, D. (1974) *J. Chem. Soc., Dalton Trans.*, 465 – 470.
[5] Maity, D., Kale, S.N., Kaul-Ghanekar, R., Xue, J.-M. and Ding, J. (2009) *J. Magnet. Magn. Mater.*, **321**, 3093 – 3098.
[6] Jankovic, B. and Mentus, S. (2009) *Metall. Mater. Trans. A*, **40**, 609 – 624.
[7] Seo, W.S., Jo, H.H., Lee, K., Kim, B., Oh, S.J. and Park, J.T. (2004) *Angew. Chem. Int. Ed.*, **43**, 1115 – 1115.
[8] Tippins, H.H. (1965) *Phys. Rev.*, **140**, A316 – A320.
[9] Binet, L. and Gourier, D. (1998) *J. Phys. Chem. Solids*, **59**, 1241 – 1245.
[10] Weh, T., Frank, J., Fleischer, M. and Meixner, H. (2001) *Sens. Actuators*, **78**, 202 – 207.
[11] Trinchi, A., Wlodarski, W. and. Li, Y.X. (2004) *Sens. Actuators, B, Chem.*, **100**, 94 – 98.
[12] Meitzner, G.D., Iglesia, E., Baumgartner, J.E. and Huang, E.S. (1993) *J. Catal.*, **140**, 209 – 225.
[13] Iwasa, N. and Takezawa, N. (2003) *Top. Catal.*, **22**, 215 – 224.
[14] Bonivaradi, A.L., Chiavassa, D.L., Querini, C.A. and Baltanas, M.A. (2000) *Stud. Surf. Sci. Catal.*, **130**, 3747 – 3752.
[15] Meriaudeau, P. and Naccache, C. (1991) *Appl. Catal.*, **73**, L13 – L18.
[16] Li, Z., de Groot, C. and Moodera, J.H. (2000) *Appl. Phys. Lett.*, **77**, 3630 – 3632.
[17] Al-Khamis, Kh.M., Al-Othman, Z.A. and Mahfouz, R.M. (2010) *Prog. React. Kinet. Mech.*, **35**, 131 – 151.
[18] Spinks, J.W.T. and Woods, R.J. (1990) *An introduction to radiation chemistry*, Wiley, New York.
[19] Sharp, J., Brindley, G. and Achar, B. (1966) *J. Am. Ceram. Soc.*, **49**, 379 – 382 .
[20] Vyzovkin, S. and Wight, C. (1999) *Thermochim. Acta*, **340 – 341**, 53 – 68.
[21] Jasim, F. (1991) *J. Therm. Anal.*, **37**, 149 – 153.